Lifetime measurement in ^{176}Lu and its astrophysical consequences

C. Doll,[1,2] H. G. Börner,[2] S. Jaag,[3] F. Käppeler,[4] and W. Andrejtscheff[5]

[1]*Technische Universität München, D-85748 Garching, Germany*

[2]*Institut Laue-Langevin, F-38042 Grenoble Cedex 9, France*

[3]*Forschungszentrum Karlsruhe, Institut für Neutronen- und Reaktorphysik, D-76021 Karlsruhe, Germany*

[4]*Forschungszentrum Karlsruhe, Institut für Kernphysik, D-76021 Karlsruhe, Germany*

[5]*Bulgarian Academy of Sciences, Institute for Nuclear Research and Nuclear Energy, 1784 Sofia, Bulgaria*

(Received 13 January 1998)

Because of its temperature-dependent half-life, ^{176}Lu represents an important thermometer for the slow neutron capture process (s process) which accounts for the origin of about half of the abundances between Fe and Bi. This interpretation of the observed ^{176}Lu abundance has been improved by a new lifetime measurement of the $J^{\pi}=5^-$ state at 838 keV in ^{176}Lu. The present limit of $\tau_{838} \geq 10$ ps provides a more stringent constraint for the thermal equilibration between the long-lived ground state ($t_{1/2}=41$ Gyr) and the short-lived K isomer at 123 keV ($t_{1/2}=3.7$ h), and, hence, for the resulting estimate of the temperature during shell helium burning in red giant stars. [S0556-2813(98)07210-0]

I. THE ^{176}Lu THERMOMETER

The main nucleosynthesis mechanisms for the heavy elements in the mass region $A \geq 56$ are neutron capture reactions in the r and s processes. For the neighborhood of Lu, the corresponding reaction paths are illustrated in Fig. 1. The rapid neutron capture process (r process) being associated with explosive, presumably supernova, scenarios is characterized by extremely high neutron densities. Consequently, the reaction path of the r process is shifted to the region of very neutron rich nuclei close to the drip line. After termination of the r process the reaction products decay back to the stability valley as indicated in Fig. 1 by inclined arrows.

For $A=176$, the β-decay chain from the r-process region is terminated at ^{176}Yb. Therefore, the r process does not contribute to the abundances of ^{176}Lu and ^{176}Hf, which can, hence, be attributed solely to the slow neutron capture process (s process) that takes place in the helium burning layers of red giant stars. This unambiguous origin in combination with the very long half-life of 41×10^9 yr [1] seemed to make ^{176}Lu a suited s-process chronometer [2,3]. Since the s abundances can be described quantitatively either by the classical approach [4] or by stellar models [5], the comparison with its present abundance was expected to yield information on the galactic history of the s process.

However, this interpretation was questioned in 1980 [6] when the role of the short-lived isomer ^{176m}Lu with a half-life of $t_{1/2}=3.68$ h was considered. This isomer at 123 keV β decays exclusively to ^{176}Hf [7] because ground state transitions are forbidden by selection rules ($\Delta I=6$, $\Delta K=7$). The critical point with this isomer was that its s-process production could not be explained in terms of the partial cross section ^{175}Lu$(n,\gamma)^{176m}$Lu, which was known from several experiments [8–10]. Instead, it was found that an additional feeding mechanism for the long-lived ground state must be invoked to account for the present ^{176}Lu abundance [7].

This additional feeding was shown to occur in the hot stellar photon bath [11] via thermally induced transitions from the isomer to a mediating state at higher excitation with a decay branch to the ground state as indicated in the schematic sketch of Fig. 2. Experimental evidence for such a state was found in detailed spectroscopic studies that resulted in a complete level scheme up to 1 MeV [12,13]. Based on these results the reaction path of the s process was discussed with emphasis on the temperature dependence of the half-life of ^{176}Lu [14], showing that this effect could, indeed, be interpreted as an s-process thermometer.

It turned out in this discussion that the coupling between isomer and ground state is not only determined by the position of the mediating state at 838 keV with $I^{\pi}=5^-$, but also by the branching ratio and, in particular, by its half-life, for which Klay $et\ al.$ [12] obtained a lower limit of $\tau \geq 2.5$ ps. In the present work, this limit is improved by a new experiment based on the gamma-ray induced Doppler broadening
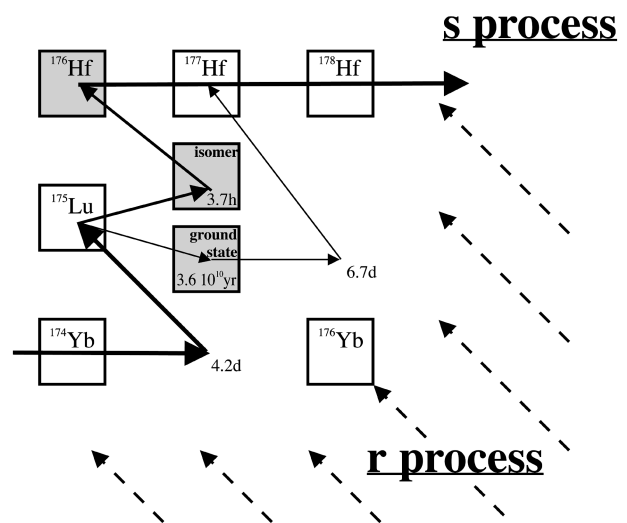

FIG. 1. The s-process neutron capture chain in the Yb-Lu-Hf region (solid lines). For ^{176}Lu, the ground state and isomer are shown separately. Note that ^{176}Lu and ^{176}Hf are shielded against r-process β decays.
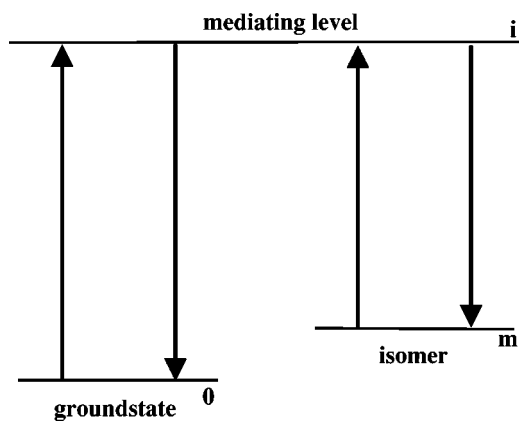
FIG. 2. The thermal coupling scheme of isomer and ground state in ^{176}Lu via thermally induced transitions to the mediating state at 838 keV.
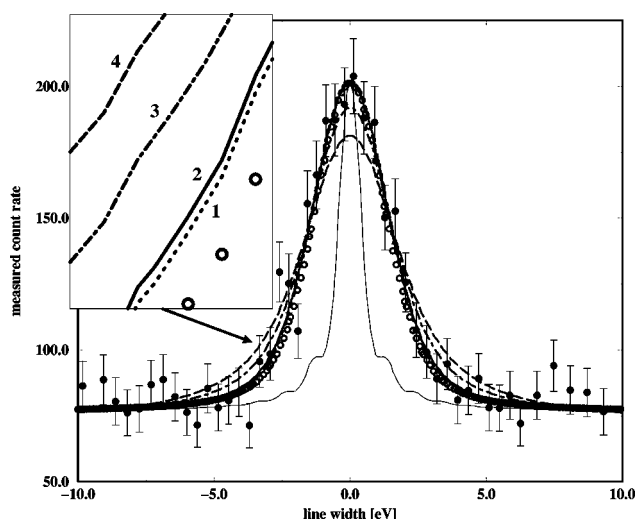

FIG. 3. The line shape of the 838 keV transition measured in third diffraction order. The inner thin line corresponds to the line-shape predicted by the dynamical diffraction theory. The circles represent the convolution of dynamical diffraction theory with the instrumental response. The dotted line (1) shows the fit for an infinite lifetime τ_{838} corresponding to the convolution of dynamical diffraction theory, instrumental response, and thermal velocity. The curves 2, 3, and 4 are obtained for lifetimes of 10, 1, and 0.5 ps, respectively.

(GRID) technique, resulting in more stringent limits for the *s*-process temperature.

II. DESCRIPTION OF THE EXPERIMENT

The lifetime of the mediating level was determined by investigating the depopulating 838 keV γ decay to the ground state via the GRID technique [15], using the two-axis flat crystal spectrometer GAMS4 [16]. This technique is based on the Doppler broadening of γ rays that are emitted in flight. After thermal neutron capture, the target nucleus finds itself in an excited state. Because of the recoil from the subsequent γ-ray emission the atom starts to move in the bulk and is gradually slowed down by collisions with the surrounding atoms. After the lifetime τ, the level of interest will be depopulated by a further γ transition. The profile of this γ-ray line is the subject of GRID investigations, its shape being broadened by several effects:

(i) the instrumental response function (experimental resolution);

(ii) the thermal motion of the nucleus with a mean velocity typical for each experiment;

(iii) the recoil provided by the feeding γ-ray transitions;

(iv) the slowing-down mechanism in the target material;

(v) the lifetime τ of the level of interest.

The determination of this broadening, which is in the order of eV for γ-ray energies in the MeV region, requires an instrument with a resolution of up to $\Delta E/E = 2 \times 10^{-6}$ which can be reached with the two-axis flat crystal spectrometer GAMS4 [16]. The usually small luminosity of this kind of instruments is compensated by the high neutron flux of the reactor at the Institut Laue-Langevin (ILL). In the present experiment, a 4.6 g sample of natural Lu_2O_3 was canned in three carbon containers, and was exposed to a neutron flux of 5×10^{14} cm^{-2} s^{-1} that is achieved at the in-pile target position in the through tube of the ILL reactor.

The first two contributions to the broadening of the line profile could be measured experimentally: the instrumental response was measured using the 838.6 keV transition in nondispersive geometry [15], and the thermal broadening was determined in dispersive geometry via the 225.4 keV level with a known lifetime of 30 ps [15]. The remaining contributions, the influence of the feeding mechanism and of the slowing-down process, have to be modeled as described below.

III. DETERMINATION OF THE LIFETIME

A. Slowing-down process

The slowing-down process is described in the mean free path approximation (MFPA) which is discussed in detail elsewhere [15]. In that model, the collisions of the excited, recoiling nucleus with the neighboring atoms are followed by due consideration of realistic interatomic distances which are derived from the Born-Mayer potential.

B. Recoil distribution

The recoil distribution is determined by the feeding pattern of the level of interest, and is, therefore, important for the evaluation of the lifetime. Whereas the feeding is rather well known for light nuclei, this is often not the case for heavy isotopes because of their higher level densities. In the odd-odd nucleus ^{176}Lu, 15% of the intensity populating the 838 keV level comes directly from the capture state and provides a feeding with an energy of 5.4 MeV. For maximum recoil, the required slowing-down time for reaching the velocity that corresponds to a given broadening is comparably long (long lifetime limit). In the opposite case of a small initial recoil, the nucleus has to emit the γ ray rapidly (small required slowing down time) in order to explain the same broadening (short lifetime limit). The present situation with 85% of the intensity originating from unknown feeding via multistep cascades has been treated by different assumptions using extreme feeding scenarios, two-step cascades, and statistical models.

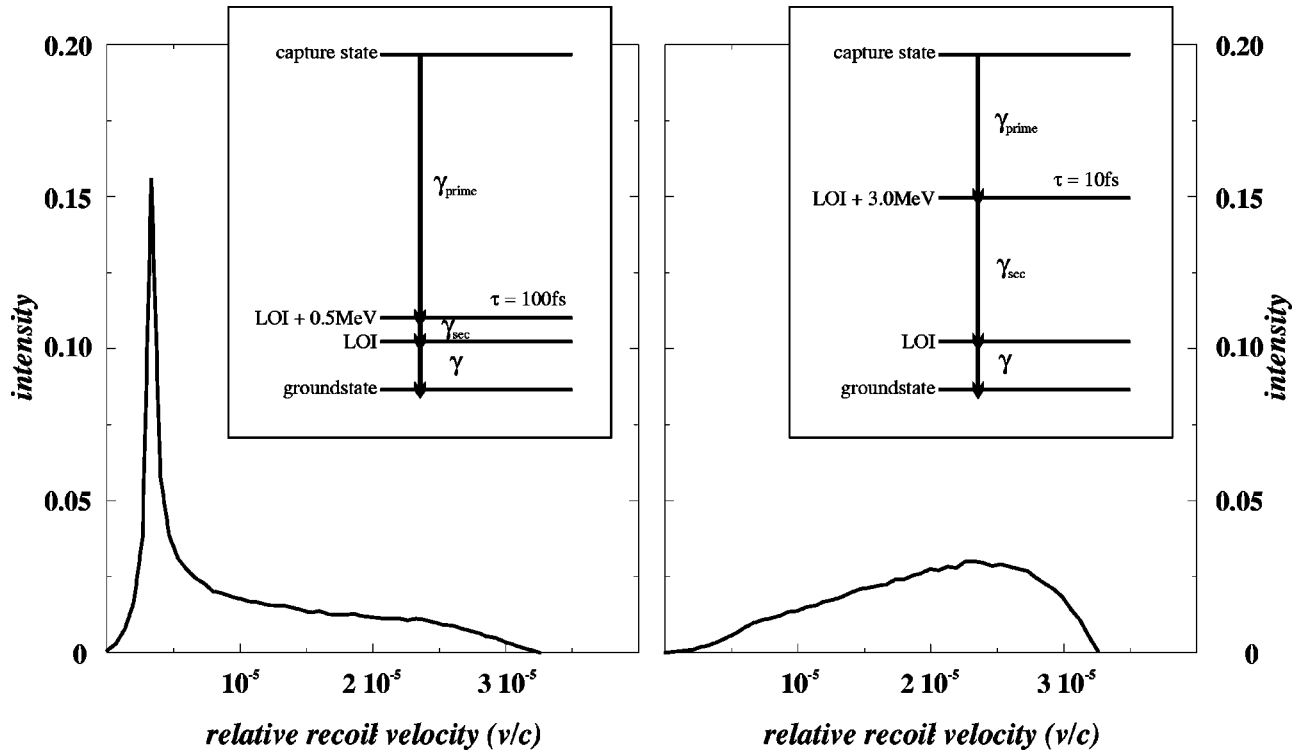Figure 3 shows the Doppler-broadened line profile of the

FIG. 4. A comparison of the two-step cascades approaches. The left-hand side shows the velocity distribution for a low-lying intermediate level with a long lifetime. Because of the long lifetime, the recoil of the primary transition is relaxed, the recoil is provided mainly by the transition from the intermediate level to the level of interest, and the velocity distribution exhibits a sharp peak at low energies (which becomes a δ function for an infinite lifetime of the intermediate level). This scenario was adopted for estimating the lower limit of the lifetime. The right-hand part shows the recoil distribution for a high-lying intermediate level with a short lifetime. Because of the short lifetime, the effect of the primary transition comes through, resulting in a smooth velocity distribution with a shift to higher velocities.

838 keV transition measured in third diffraction order. It is evident that the lifetime of this level has only a very small effect on the broadening of the line which means that this case is already close to the upper limit of the GRID method. Therefore, the feeding problem is particularly important and requires to be discussed in detail.

1. Extreme feeding scenarios and two step cascades

Since the Doppler profile depends on the recoil velocity distribution at the moment when the level in question is populated, it is directly determined by the transitions that are feeding this level. In principle, this problem can be treated by using feeding transitions with given energies, which originate from levels with given lifetimes. The main difficulty is to vary the lifetimes of these intermediate levels and the energies of the corresponding transitions in a proper way. For estimating limits, the level scheme of Klay *et al.* [12] was adopted for the input of the known feeders. In order to give an impression on how the lifetime depends on the feeding scenario we start with the assumption (for the unobserved population), that an extreme limit for the lifetime can be obtained if our level is populated by a low-energy transition—say, 500 keV—originating from a level with an infinite lifetime. Taking the uncertainties of the instrumental resolution and thermal velocity into account, such an extreme case would yield a value of $\tau_{838} \geq 1.3$ ps (see Table II).

A more realistic approach is obtained by using a generalized two-step cascade description. It was assumed that the

capture state is depopulated by a γ transition to an intermediate level from which the level of interest is fed. The lifetime and the energy of this intermediate level was varied and the resulting recoil distributions have been used for deducing the lifetime.

Figure 4 illustrates the influence of the properties of the intermediate level for this feeding scenario in more detail. Variation of the energy and the lifetime of the intermediate level result in very different recoil distributions. The left panel of Fig. 4 demonstrates the effect of a long-lived low-lying intermediate level. Because of the long lifetime, the recoil of the primary transition is relaxed and the transition from the intermediate level to the level of interest provides a comparably small recoil to the nucleus. Hence, the corresponding velocity distribution shows a sharp peak at low energies and a δ function for $\tau_{\text{intermediate}} \to \infty$. By comparison with the experimentally determined broadening, this small initial velocity results in a short lifetime.

On the right panel of Fig. 4 the recoil distribution for a high-lying intermediate level with a short lifetime is shown. Because of the short lifetime, the effect of the previous—or for instance primary—transitions comes through, resulting in a broader distribution with a shift to higher velocities. In this case, the nucleus gets a rather large initial recoil velocity. For the given experimental broadening, this leads to a long lifetime. The χ^2 distributions for a variation of the intermediate level energy in the range of 0.5–5 MeV above the level of interest and assumed lifetimes between 0 and ∞ are shown in Fig. 5. The three isolated curves on the left side of
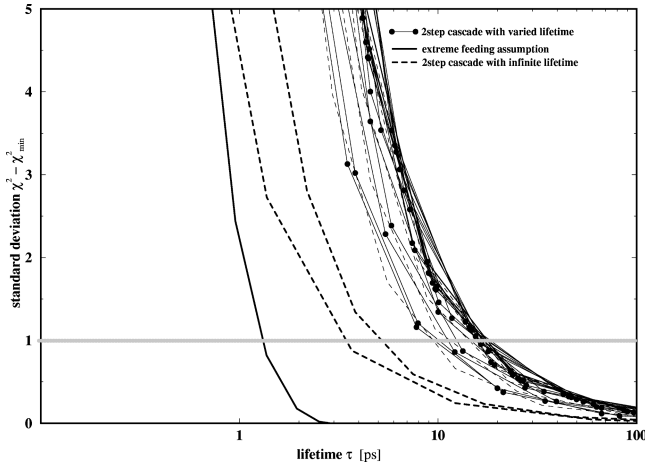
FIG. 5. The χ^2 distribution from the fit of the line shape of the 838 keV transition as a function of the lifetime τ_{838}. On the left-hand side results from the extreme feeding assumptions with an infinite intermediate level lifetime are shown (for feeders of 0.5, 1.0, and 1.5 MeV). The distribution for an intermediate level energy of 0.5 MeV corresponds to a (very unrealistic) lower limit τ_{min}. The curves on the right hand side were obtained for intermediate level energies between 2 and 5 MeV and lifetimes ranging from 0 to ∞ as well as for lifetimes between 0 and 100 fs for feeding transitions of 1 and 1.5 MeV. The left envelope of this bulk corresponds to a limit of $\tau_{838} \geqslant 10$ ps for these two step cascades.

the figure represent an infinite lifetime of the intermediate level and the feeding corresponds to one transition only (where the total missing intensity is represented by a δ function in the velocity distribution) with energies of 0.5, 1.0, and 1.5 MeV, respectively. This situation can be postulated as highly unprobable because here we approach a situation where the feeding comes from a (so far unobserved) isomeric state. Also, the probability for a low-lying state decaying by 100% to our level, is low. When we exclude these unprobable scenarios the results obtained (Fig. 5) approach the statistical feeding results (Fig. 6) with a 1σ limit of $\tau_{838} \geqslant 10$ ps.

2. Statistical models

In the statistical simulations, two approaches were employed, cascade feeding simulations using the code GALENA [17], which includes the constant temperature Fermi-gas formalism, and a statistical model developed by Becvar et al. [18] using the computer code DICEBOX. This second model is based on the complete knowledge of all experimental established nuclear levels. ''Missing'' levels are constructed via the random discretization of a level density formula. The lifetimes of the resulting levels are deduced from a Porter-Thomas distribution by due consideration of the photon strength functions. The feeding pattern itself is generated by the Monte Carlo method resulting in initial velocity distributions for the level of interest.

C. Results

The measured lineshape corresponds to a convolution of the instrumental response, the broadening due to the thermal movement of the target atoms as well as the recoil induced by feeding of the level of interest and its lifetime τ. The line
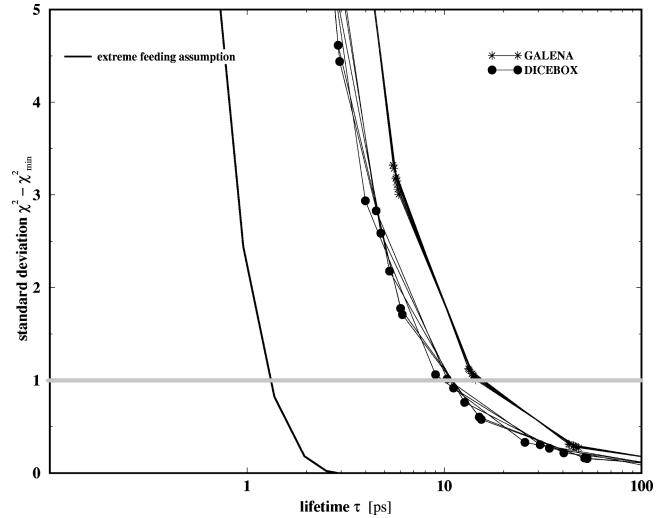

FIG. 6. The χ^2 distributions from the fit of the line shape of the 838 keV transition as a function of the lifetime τ_{838}. The two sets of curves are obtained with the statistical models. To guide the eye the 0.5 MeV limit from extreme feeding assumptions is also included in the figure.

shapes were fitted by means of the code GRIDDLE [19] with the lifetime τ_{838} of the mediating state as a free parameter. Altogether we have measured this transition 17 times (using several reflection orders) in order to obtain very good statistics. It is obvious from Fig. 3 that in the case considered here the effect due to the lifetime is small compared to the contributions from thermal broadening and instrumental response, resulting in a lower limit of the lifetime.

This is demonstrated in Fig. 3, which compares calculated Doppler profiles for fixed lifetimes of the level of interest with the measured lineshape. A best fit (the minimum in χ^2) is found for an infinite lifetime τ_{838} of the mediating level. In Table I the corresponding χ^2 differences from the fit to a lifetime $\tau_{838} \rightarrow \infty$ are given. The 10 ps limit is derived from a 1σ deviation. The 2σ limit corresponds to a lifetime τ_{838} of about $\geqslant 5.5$ ps, 3σ gives a lifetime limit of about $\geqslant 4$ ps, and this grows rapidly to 58σ for a lifetime τ_{838} of 0.5 ps. It is obvious from Fig. 3 that lifetimes of 0.5 ps or 1 ps correspond to profiles which deviate clearly from the measured lineshape. For this example, the assumption of a two step cascade was used with an intermediate level lifetime of 100

TABLE I. The deviations $\Delta\sigma$ from the χ^2 minimum for different fixed lifetimes τ_{838}. The assumption of a two step cascade was combined with an intermediate level of 100 fs lifetime located 1.5 MeV above the level of interest, corresponding to the left rim of the bulk of $\chi^2(\tau)$ curves in Fig. 5.

Fixed lifetime τ	Deviation from χ^2_{min}
	$\Delta\sigma$
0.5 ps	58
1.0 ps	21
4.0 ps	3
5.5 ps	2
10 ps	1
$\tau \rightarrow \infty$	0

TABLE II. Lifetime values of the relevant mediating level in ^{176}Lu at 838 keV obtained with the assumptions of an extreme feeding scenario, a two step cascade, and using statistical models. The lower limit accounts for the experimental uncertainties of instrumental response and thermal velocity.

	Two step cascade		Statistical models	
	(extreme feeding)	variations in τ and E	DICEBOX	GALENA
Lifetime τ (ps)	1.3	~ 10	10	10.5

fs and an intermediate level energy of 1.5 MeV above the level of interest. This situation is very close to the envelope of the statistical model description (see Fig. 6) but without the big demand in computing time.

The various contributions described in Sec. II are also illustrated in Fig. 3. The thin line shows the line profile predicted by dynamical diffraction theory. This profile is folded with a Gaussian contribution which accounts for the instrumental response (open circles). The dotted line shows the instrumental response folded with the thermal velocity of the target atoms, corresponding to a profile for a lifetime $\tau = \infty$, which represents the best fit. A finite lifetime of our 838 keV state would show up as an additional broadening.

The fitting routine used in GRIDDLE is scanning the χ^2 plane for a minimum in a standard way (Marquart-Levenberg algorithm [19]). In the case of the 838 keV transition, the resulting $\chi^2(\tau)$ function is asymmetric and steeply decreasing in the ps region without providing a "real" minimum (Figs. 5 and 6). Accordingly, a unique solution of the fit and thus a clear lifetime value is not reached.

Instead, a lower limit $\tau_{\min}$ can be deduced from the minimal χ^2 value: $\chi^2(\tau_{\min}) = \chi^2_{\min} + 1$. Fig. 5 shows the $\chi^2(\tau)$ curves for the extreme feeding assumption and for the more realistic two-step cascades. With the statistical models (Fig. 6), a lower limit of $\tau_{\min} = 10$ ps and $\tau_{\min} = 10.5$ ps, respectively, is obtained, in good agreement with the value based on the assumptions for the two-step cascades.

All results are listed in Table II. If the values obtained with the very extreme feeding assumptions—which are far from being realistic but provide absolute limits based on the knowledge of the level scheme—are excluded, the present GRID measurement and the simulations using the two-step cascade picture and the statistical models yield a final lower limit

$$\tau_{838} \geqslant 10 \text{ ps },$$

which represents a considerable improvement over the previous best estimate of 2.5 ps [14]. Together with the upper limit determined via the generalized centroid-shift method [12], the present experimental limits for the lifetime of the mediating level in ^{176}Lu are

$$10 \text{ ps} \leqslant \tau_{838} \leqslant 300 \text{ ps}.$$

IV. THEORETICAL LIFETIME ESTIMATES

The level at 838.6 keV is the $J^\pi = 5^-$ member [14] of the $K^\pi = 4^-$ band based on the proton-neutron configuration $p 1/2^+[411] + n 7/2^-[514]$. It decays to several lower-lying levels with a total intensity of $I_{tot} = 4.42$ per 100 captured neutrons including to the $J^\pi = 4^-$ band head at 722.9 keV by

a transition of 115.7 keV of (predominantly) $M1$ multipolarity. This transition is weak ($I_\gamma = 0.09, I_{tot} = 0.315$) and in the conversion-electron measurements [14] an $E2$ component could not be quantitatively established. However, such a component must be present in any $\Delta J = 1$ rotational transition in a well-deformed nucleus (provided the relevant Clebsch-Gordan coefficients do not vanish like in a $K = 0$ band). The corresponding reduced transition probability reads

$$B(E2) = \frac{5}{16\pi} \langle J_i K 20 | J_f K \rangle^2 Q_0^2 e^2. \tag{1}$$

With $Q_0 = 7.1$ b, $B(E2) = 1.64 \ e^2 \text{ b}^2$, resulting in a partial γ-ray lifetime $\tau^\gamma(E2) = 2.4$ ns for the 115.7 keV transition. Assuming 100% $E2$ decay [i.e., $\tau^\gamma(M1) = \infty$] and taking into account the relative γ-ray intensities [14] as well as the conversion-electron coefficients [20] (see Ref. [21] for the corresponding expressions), an *extreme upper limit* of $\tau_{838} \approx 50$ ps is estimated for the lifetime of this level. Hereby, the relation between the total partial γ-ray lifetime of a transition τ^γ_{tr} and those of its components (here $M1$ and $E2$) is

$$\frac{1}{\tau^\gamma_{tr}} = \frac{1}{\tau^\gamma(M1)} + \frac{1}{\tau^\gamma(E2)}. \tag{2}$$

It is clear from this relation that any $M1$ component [i.e., a finite $\tau^\gamma(M1)$] would enhance the transition, thus reducing the estimated lifetime τ_{838} to 25 ps (for 50% $E2$), 5 ps (10% $E2$), and 2.5 ps (5% $E2$), respectively. The measured K-conversion coefficient for the 115.7 keV transition is even somewhat larger than the theoretical value for multipolarity $M1$ which is in turn larger than the theoretical $E2$ K-conversion coefficient. This implies that the $E2$ component of this transition is certainly small. Unfortunately, L-conversion lines could not be analyzed to establish the $E2/M1$ mixing ratio δ^2 [$\delta^2 = \tau^\gamma(M1)/\tau^\gamma(E2)$]. Nevertheless, it appears sufficiently safe to *assume* a composition of 50% $M1 + 50\%$ $E2(\delta^2 = 1)$, yielding a *realistic upper limit* of $\tau_{838} \approx 25$ ps.

It is to be noted that this is based only on the well-established collective-model relation concerning rotational $E2$ transitions. Predictions for the unknown mixing ratio δ^2 can be obtained by additional model calculations of the $M1$ transition probability. Within a rotational band of a doubly odd deformed nucleus, the reduced $M1$ transition probability is determined [22] by the expression

$$B(M1) = \frac{3}{4\pi} \langle J_i K 10 | J_f K \rangle^2 (G^{KK})^2 \mu_N^2, \tag{3}$$

where

$$G^{KK} = [\Omega_p(g_{\Omega_p} - g_R) + \Omega_n(g_{\Omega_n} - g_R)]. \qquad (4)$$

In the present case, $\Omega_p = 1/2$ and $\Omega_n = 7/2$. The corresponding odd-particle gyromagnetic ratios $g_p(1/2^+[411]) = 3.03$ and $g_n(7/2^-[514]) = 0.28$ were calculated in the frame of the Nilsson model [23] with a deformation parameter $\epsilon_2 = 0.27$ and the usual quenching $g_s^{eff} = 0.7 g_s^{free}$ assuming axial symmetry and neglecting higher-order deformations. If the collective gyromagnetic ratio g_R was varied in the reasonable interval between 0.3 and 0.45 [22], the $E2$ component is predicted to range between 19% and 44%, producing level lifetimes between 9 and 23 ps. Hence, the model calculations reasonably confirm the experimental expectations.

In Ref. [22], semiempirical g factors of several orbitals in strongly deformed odd-odd nuclei are derived from experimental branching ratios and magnetic moments. The values of interest for the present estimate are given there as $g_p(1/2^+[411]) = 1.65$ and $g_n(7/2^-[514]) = 0.155$. With these values and with g_R again in the range of 0.3–0.45, considerably smaller reduced transition probabilities $B(M1)$ are obtained than in the Nilsson model (i.e., unrealistic $\delta^2 \geqslant 2$), giving rise to lifetimes closer to the extreme upper limit of 50 ps.

There are some nuclear structure problems arising from this estimate, e.g., the unusually large strength (~ 1 W.u. at $\tau_{lev} = \sim 20$ ps) of the K-forbidden $E2$ transition of 838.6 keV linking this level with the $J^\pi K = 77^-$ ground state $p7/2^+[404] + n7/2^-[514]$. It appears rather striking that with $I_\gamma = 3.4$ this out-of-band transition by far dominates the depopulation of the rotational level under investigation. The consideration of these problems is, however, beyond the scope of the present work.

In conclusion, the estimates made on the basis of the level scheme [14] within the rotational model point at a lifetime of the 838.6 keV level which is certainly below 50 ps, probably close to the lower experimental limit of 10 ps.

V. THE s-PROCESS TEMPERATURE

The s process at mass number $A = 176$ is determined by the competition between β decay of the short-lived isomer and neutron capture in the long-lived ground state, resulting in a branching in the reaction flow as shown in Fig. 1. Following the notation of Klay *et al.* [14], the feeding of the long-lived ^{176}Lu ground state can be described by the branching factor f_n:

$$(\sigma N)_{176_{Lu}} = f_n[(\sigma N)_{176_{Lu}} + (\sigma N)_{176_{Hf}}],$$

where σN denotes the product of stellar neutron capture cross section σ and the respective abundance produced by the s process.

For ^{176}Lu, this branching factor is determined by the partial cross sections feeding the isomer and the ground state as well as by the thermal coupling of these two states via the mediating level at 838 keV. According to this complex situation, f_n depends on neutron density n_n and temperature T [14]
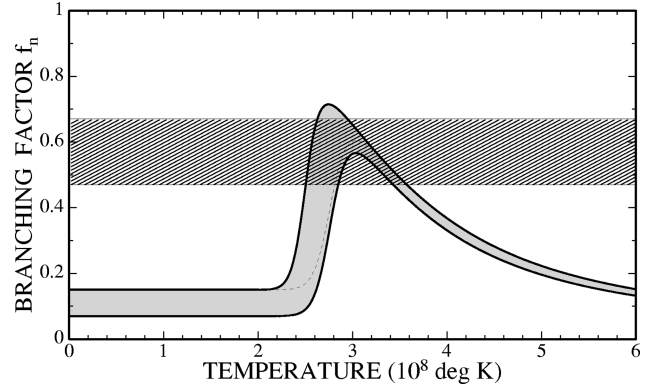

FIG. 7. The branching factor f_n as a function of temperature (shaded band) compared with the effective branching factor (hatched band), which was obtained by means of the classical s-process model. The transition between the low-temperature regime, characterized by the initial neutron capture production of ^{176}Lu, and the high-temperature regime with complete thermal equilibrium occurs between 250 and 350 million K (for details see text).

$$f_n^{-1}(n_n, T) = 1 + \frac{\lambda_\beta^{(m)}}{\lambda_n} \frac{p_m}{p_0},$$

where $\lambda_\beta^{(m)}$ denotes the decay rate of the isomer, $\lambda_n = \sigma v_T n_n$ the neutron capture rate of the ground state, and p_m, p_0 the respective population probabilities. These probabilities are

$$p_m = \frac{V(1-V)}{\tau_i} \frac{g_i}{g_0} \exp[-E_i/kT] + (1-B)\sigma v_T n_n$$

and

$$p_0 = \frac{V(1-V)}{\tau_i} \frac{g_i}{g_m} \exp[-(E_i - E_m)/kT] + B\lambda_\beta^{(m)},$$

v_T being the mean thermal velocity.

Apart from the properties of the mediating state (branching ratio V, lifetime τ_i, statistical factor g_i, and excitation energy E_i), these expressions are mostly determined by the Boltzmann factors for excitation of the mediating level E_i from the ground state or from the isomer. The quantity

$$B = \frac{\sigma^{(g)}}{\sigma_{total}} = 0.11 \pm 0.04$$

corresponds to the partial capture cross section of ^{175}Lu to the ground state in ^{176}Lu [10].

With the present best estimate of the s-process neutron density $n_n = (4.1 \pm 0.6) \times 10^8$ cm^{-3} [24] the above expressions yield the branching factor as a function of stellar temperature as shown by the shaded band in Fig. 7 (which provides an update of Fig. 5 in Ref. [14]). The upper and lower limits of the shaded band correspond to the present value of the lifetime $\tau_{838} = 10$ ps and to the upper and lower bounds for the neutron density n_n and for the feeding ratio B. For comparison, the dashed line illustrates the effect of the upper limit of 300 ps for τ_{838}. Since the difference to the 10 ps limit is similar to the width of the shaded band, which results

from the uncertainties in n_n and B, further improvements of τ_{838} should also be complemented by an improvement of those parameters.

The temperature behavior of the branching factor differs significantly in the following three regions:

(i) At low temperatures, f_n is completely defined by the ratio B, i.e., by the partial capture cross section feeding the ground state. Induced internal transitions are too weak and have negligible effect on the branching.

(ii) Between 240 and 300 million degrees, thermally induced transitions cause drastic changes in the population probabilities of ground state and isomer, resulting in an enhanced feeding of the ground state. It is due to this effect that more ^{176}Lu is observed in nature than would be created in a ''cool'' environment. In this regime, internal transitions, β decays, and neutron captures are equally important.

(iii) For temperatures above 300 million degrees, thermal equilibrium in the relative population of ground state and isomer is eventually established, internal transitions being now much faster than the time scales for β decay and neutron capture. Accordingly, f_n is decoupled from the initial branching ratio B.

The hatched band in Fig. 7 indicates the limits for the effective value of f_n that results independently from an empirical analysis of the s-process flow via the so-called classical approach. The combined information of the σN value for $A = 176$ as obtained from the overall systematics in combination with the respective σN values for ^{176}Lu and ^{176}Hf yields [14]

$$f_n = 0.57 \pm 0.10.$$

The overlap between this effective value and the temperature-dependent branching factor provides an even higher limit for the s-process temperature

$$2.5 \times 10^8 \leqslant T \leqslant 3.5 \times 10^8 \text{ K},$$

compared to the previous study of Ref. [14].

This result is particularly important with respect to current stellar models. In these models, the *main s-process component*, which accounts for the s abundances in the mass region $90 \leqslant A \leqslant 209$, is assumed to operate during helium shell burning in thermally pulsing stars on the asymptotic giant branch (AGB stars) of the Hertzsprung-Russell diagram [5]. In this scenario, neutron production and concordant s processing occur in two steps, by the ^{13}C$(\alpha,n)^{16}$O reaction during the hydrogen-burning stage at relatively low temperatures of $T \approx 1 \times 10^8$ K and during the subsequent helium burning by the ^{22}Ne$(\alpha,n)^{25}$Mg reaction at $T \approx 3 \times 10^8$ K.

From the present result it is obvious that ^{176}Lu is underproduced at the low temperatures of the first phase. This

deficiency must, therefore, be compensated during the helium-burning phase where the s process operates at higher temperatures. In this respect, the observed ^{176}Lu abundance can be used to constrain the temperature as well as the neutron exposure of this later episode.

VI. SUMMARY

The interpretation of ^{176}Lu as a stellar thermometer has been improved by a measurement of the lifetime for the relevant mediating state that provides the thermal coupling between the long-lived ground state and the short-lived isomer. The experiment was carried out via the GRID technique by measuring the line profile of the ground state transition from the mediating state at 838 keV excitation energy with a resolution of 3.2 eV. From the measurement of this line a lower limit of 10 ps could be inferred for the lifetime, 4 times longer than the previous limit [14].

The analysis in terms of an s-process thermometer followed the approach described by Klay *et al.* [14] but made use of the present result and of an improved estimate for the s-process neutron density [24]. The resulting temperature limits confirm that ^{176}Lu provides, indeed, a firm *lower* limit for the effective s-process temperature, which has now been determined to 2.5 GK.

This value represents an important condition for stellar s-process models, which are currently related to helium shell burning in low mass AGB stars [5]. This scenario is characterized by the subsequent activation of two neutron sources, the ^{13}C(α,n) and the ^{22}Ne(α,n) reactions, which operate at very different temperatures of 1×10^8 K and 3×10^8 K, respectively. While not enough ^{176}Lu can be produced at the lower temperature, the relative neutron exposure during the high-temperature episode can, hence, be constrained by the observed abundance value.

It has to be noted, however, that this interpretation of the thermal coupling between ground state and isomer considers only allowed transitions to and from the mediating level. The role of K-forbidden transitions from lower states has been discussed by Klay *et al.* [14] who found this effect to be of minor importance.

[1] R. Gehrke, C. Casey, and R. Murray, Phys. Rev. C **41**, 2878 (1990).

[2] J. Audouze, W. Fowler, and D. Schramm, Nature **238**, 8 (1972).

[3] M. Arnould, Astron. Astrophys. **22**, 311 (1973).

[4] F. Käppeler, H. Beer, and K. Wisshak, Rep. Prog. Phys. **52**, 945 (1989).

[5] R. Gallino *et al.*, Nucl. Phys. **A621**, 423c (1997).

[6] R. Ward, private communication (unpublished).

[7] H. Beer, G. Walter, R. Macklin, and P. Patchett, Phys. Rev. C **30**, 464 (1984).

[8] B. Allen, G. Lowenthal, J. Boldeman, and J. de Laeter, in *Neutron Capture Gamma-Ray Spectroscopy and Related Topics*, edited by T. von Egidy, F. Gönnenwein, and B. Maier

(Institute of Physics, Bristol, 1982), p. 573.

[9] F. Stecher-Rasmussen *et al.*, in *Capture Gamma-Ray Spectroscopy 1987*, edited by K. Abrahams and P. Van Assche (Institute of Physics, Bristol, 1988), p. 754.

[10] W. Zhao and F. Käppeler, Phys. Rev. C **44**, 506 (1991).

[11] H. Beer, F. Käppeler, K. Wisshak, and R. Ward, Astrophys. J., Suppl. Ser. **46**, 295 (1981).

[12] N. Klay *et al.*, Phys. Rev. C **44**, 2801 (1991).

[13] K. Lesko *et al.*, Phys. Rev. C **44**, 2850 (1991).

[14] N. Klay, F. Käppeler, H. Beer, and G. Schatz, Phys. Rev. C **44**, 2839 (1991).

[15] H. Börner and J. Jolie, J. Phys. G **19**, 217 (1993).

[16] M. Dewey *et al.*, Nucl. Instrum. Methods Phys. Res. A **284**, 151 (1989).

[17] B. Krusche (unpublished).

[18] F. Becvar *et al.*, in *Measurement, Calculation and Evaluation of Photon Producing Data*, edited by C. Coceva, A. Mengoni, and A. Ventura (E.N.E.A., Bologna, 1994), p. 81.

[19] S. Robinson and J. Jolie, Technical Report, Institut Laue-Langevin (unpublished).

[20] F. Rösel, H. Fries, K. Alder, and H. Pauli, At. Data Nucl. Data Tables **21**, 91 (1978).

[21] W. Andrejtscheff, K. Schilling, and P. Manfrass, At. Data Nucl. Data Tables **16**, 515 (1975).

[22] J. Kern and G. Struble, Nucl. Phys. **A286**, 371 (1977).

[23] S. Larsson, G. Leander, and I. Ragnarsson, Nucl. Phys. **A307**, 189 (1978).

[24] K. Toukan, K. Debus, F. Käppeler, and G. Reffo, Phys. Rev. C **51**, 1540 (1995).